

## LETTERS

# Functional diversification of closely related ARF-GEFs in protein secretion and recycling

Sandra Richter<sup>1</sup>, Niko Geldner<sup>1†</sup>, Jarmo Schrader<sup>1</sup>, Hanno Wolters<sup>1</sup>, York-Dieter Stierhof<sup>2</sup>, Gabino Rios<sup>3†</sup>, Csaba Koncz<sup>3</sup>, David G. Robinson<sup>4</sup> & Gerd Jürgens<sup>1</sup>

Guanine-nucleotide exchange factors on ADP-ribosylation factor GTPases (ARF-GEFs) regulate vesicle formation in time and space by activating ARF substrates on distinct donor membranes<sup>1</sup>. Mammalian GBF1 (ref. 2) and yeast *Gea1/2* (ref. 3) ARF-GEFs act at Golgi membranes, regulating COPI-coated vesicle formation. In contrast, their *Arabidopsis thaliana* homologue GNOM (GN) is required for endosomal recycling, playing an important part in development<sup>4</sup>. This difference indicates an evolutionary divergence of trafficking pathways between animals and plants, and raised the question of how endoplasmic reticulum–Golgi transport is regulated in plants. Here we demonstrate that the closest homologue of GNOM in *Arabidopsis*, GNOM-LIKE1 (GNL1; NM\_123312; At5g39500), performs this ancestral function. GNL1 localizes to and acts primarily at Golgi stacks, regulating COPI-coated vesicle formation. Surprisingly, GNOM can functionally substitute for GNL1, but not vice versa. Our results suggest that large ARF-GEFs of the GBF1 class perform a conserved role in endoplasmic reticulum–Golgi trafficking and secretion, which is done by GNL1 and GNOM in *Arabidopsis*, whereas GNOM has evolved to perform an additional plant-specific function of recycling from endosomes to the plasma membrane. Duplication and diversification of ARF-GEFs in plants contrasts with the evolution of entirely new classes of ARF-GEFs<sup>5</sup> for endosomal trafficking in animals, which illustrates the independent evolution of complex endosomal pathways in the two kingdoms.

Large ARF-GEFs are represented by two subfamilies conserved among eukaryotes: the GBF1 clade, including mammalian GBF1, yeast *Gea1/2* and *Arabidopsis* GNOM; and the BIG clade, including mammalian BIG1/2, yeast *Sec7* and *Arabidopsis* BIG1–5 (refs 5, 6) (Fig. 1a). Whereas GBF1 and *Gea1/2* have been localized to the Golgi<sup>2,3,7</sup>, and a double knockout for *Gea1/2* is cell-lethal<sup>5,7</sup>, GNOM performs a plant-specific endosomal recycling function important for development but not essential for cell viability<sup>4,8,9</sup>. Large ARF-GEFs are the molecular targets for brefeldin A (BFA), which causes reversible inhibition of vesicle trafficking<sup>4</sup>. BFA traps sensitive ARF-GEFs on the membrane by blocking the guanine-nucleotide exchange reaction<sup>10</sup>. BFA sensitivity or resistance can be engineered by site-directed mutagenesis, without affecting protein function<sup>11</sup>, providing a unique tool to selectively inhibit specific ARF-GEFs to probe their function *in vivo*. This approach revealed that GNOM is involved in endosomal recycling of PIN1, a polarly localized component of auxin efflux carriers<sup>4</sup>. We now extend this approach to identify the ARF-GEF responsible for endoplasmic reticulum (ER)–Golgi trafficking. BFA was shown to cause the release of COPI coats from membranes in mammalian cells<sup>12,13</sup>. In *Arabidopsis*, however, BFA treatment has no effect on Golgi structure

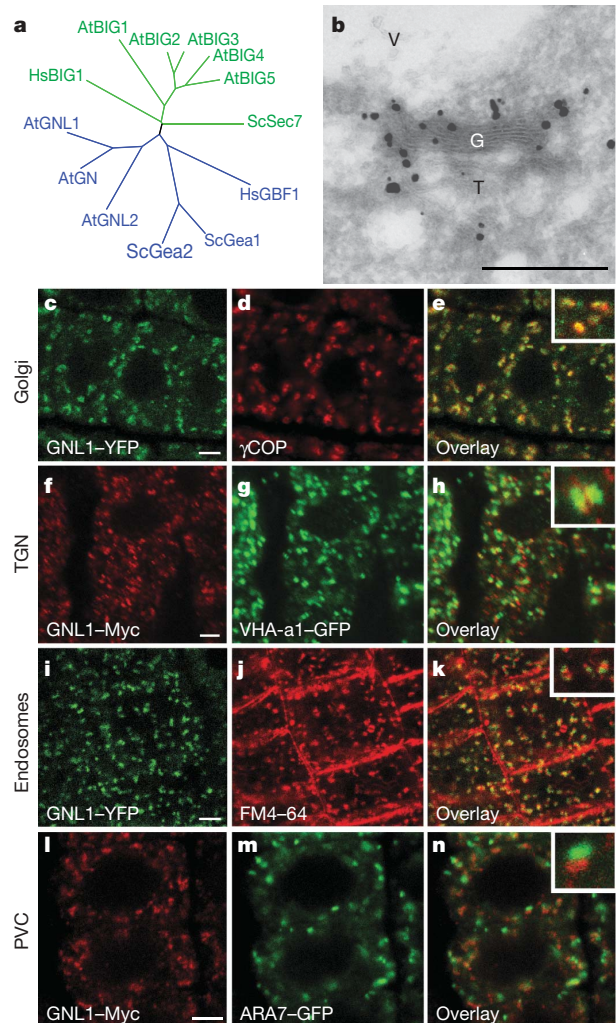


**Figure 1 | Identification of the GNL1 compartment.** **a**, Unrooted phylogenetic tree of large ARF-GEFs from *Arabidopsis* (At), human (Hs) and yeast (Sc). **b**, Immunogold localization of GNL1–YFP on an ultrathin cryosection. G, Golgi; T, TGN; V, vacuole. Scale bar, 500 nm. **c–n**, Immunofluorescence localization of GNL1 and endomembrane markers. Scale bars, 4  $\mu$ m. **c–e**, GNL1–YFP partially colocalizes with Golgi marker  $\gamma$ COP. No colocalization was observed for GNL1–Myc and TGN marker VHA–a1–GFP (**f–h**), GNL1–YFP and endocytic tracer FM4–64 (**i–k**) or GNL1–Myc and prevacuolar compartment marker ARA7–GFP (**l–n**).

<sup>1</sup>ZMBP, Entwicklungsgenetik, and <sup>2</sup>ZMBP, Mikroskopie, Universität Tübingen, Auf der Morgenstelle 3, D-72076 Tübingen, Germany. <sup>3</sup>Max-Planck-Institut für Pflanzenzüchtung, Carl-von-Linné-Weg 10, D-50829 Köln, Germany. <sup>4</sup>Department of Cell Biology, Heidelberg Institute for Plant Sciences, University of Heidelberg, D-69120 Heidelberg, Germany. <sup>†</sup>Present addresses: Salk Institute for Biological Studies, La Jolla, California 92037, USA (N.G.); Departamento Bioquímica y Biología Molecular, Facultad Biología, Universidad de Valencia, E-46100 Burjassot, Spain (G.R.).

or membrane association of the COPI subunit  $\gamma$ COP<sup>4,14</sup>, suggesting that a BFA-resistant ARF-GEF mediates this process. Evident candidates are the two closest homologues of GNOM. We decided to focus on ubiquitously expressed GNOM-LIKE1 (GNL1) because GNL2 seems to be pollen-specific<sup>15</sup> (Supplementary Fig. 2).

To identify the endomembrane compartment at which GNL1 acts, we generated plants expressing functional GNL1-Myc or GNL1-YFP (yellow fluorescent protein). GNL1 was localized relative to compartment-specific markers (Fig. 1; Supplementary Table 1). GNL1 partially co-localized with the Golgi marker  $\gamma$ COP<sup>16</sup> but did not, or only marginally so, with the *trans*-Golgi network (TGN) marker VHA-a1-GFP<sup>17</sup>, which was consistent with the immunogold-localization of GNL1 (Fig. 1b–h; Supplementary Fig. 3f). In contrast, GNL1 did not co-localize with ARA7-GFP labelling endosomes/pre-vacuolar compartments<sup>18,19</sup> nor the endocytic tracer FM4-64 (ref. 4) (Fig. 1i–n). These results suggest a role for GNL1 in Golgi-related trafficking.

BFA treatment of *Arabidopsis* seedlings causes aggregation of endosomal membrane vesicles (so-called BFA compartments), to which GNOM has been localized<sup>4,14</sup>. Predominantly at the periphery of BFA compartments, GNL1 partially co-localized with the Golgi markers  $\gamma$ COP and N-ST-YFP<sup>20</sup>, and also overlapped with VHA-a1-GFP and FM4-64 (Fig. 2a–d; Supplementary Fig. 4). To conditionally inactivate GNL1 by BFA treatment, we introduced an engineered BFA-sensitive GNL1 into a *gnl1* knockout background. This switch to BFA-sensitivity of GNL1 caused a dramatic change in BFA effects. We now observed a release of  $\gamma$ COP into the cytosol and a block in ER–Golgi traffic, as highlighted by the accumulation of the Golgi marker N-ST-YFP in the ER as well as the fusion of Golgi stacks with the ER (Figs 2g, h and 3c, d; Supplementary Fig. 3). Consistently, BFA-sensitive GNL1 localized to the ER but also co-localized with FM4-64 in BFA compartments (Fig. 2f; Supplementary Fig. 5; see Supplementary Fig. 3g and h for immunogold localization of GNL1-YFP). This indicates that GNL1 activity is required for the integrity of Golgi stacks and for COPI-coated vesicle formation. To analyse whether GNL1 might also have another role in trafficking, we studied the membrane association of another major vesicle coat protein, clathrin (Supplementary Fig. 6). In contrast to  $\gamma$ COP, however, clathrin was not released into the cytosol by BFA treatment of BFA-sensitive GNL1, which is consistent with the localization of GNL1 and clathrin to adjacent but distinct compartments (Supplementary Fig. 6a–c, g–i). As a consequence of blocking anterograde traffic of newly synthesized proteins from the ER to the Golgi, the TGN marker VHA-a1-GFP also accumulated at the ER (Fig. 2i). Thus, GNL1 is a major regulator of ER–Golgi trafficking and protein secretion.

If GNL1 has such an important role in membrane traffic one would expect inactivation of the *GNL1* gene to be lethal. We identified a T-DNA insertion knockout line for *GNL1* (Supplementary Fig. 7a). Surprisingly, the *gnl1* mutant plants were viable and fertile—although short and bushy—and pollen competitiveness was reduced to 76% (Fig. 3i). Another strong allele, *gnl1-2*, isolated as a secretion mutant, showed a very similar phenotype (ref. 21; our unpublished

observations). These results indicate that GNL1 is not essential. Consistently, *gnl1* mutant cells displayed slightly abnormal Golgi stacks with cisternae laterally expanded by approximately 35% (Fig. 3a, b; Supplementary Fig. 3i). However, BFA treatment of *gnl1* mutant cells caused fusion of the Golgi with the ER, suggesting

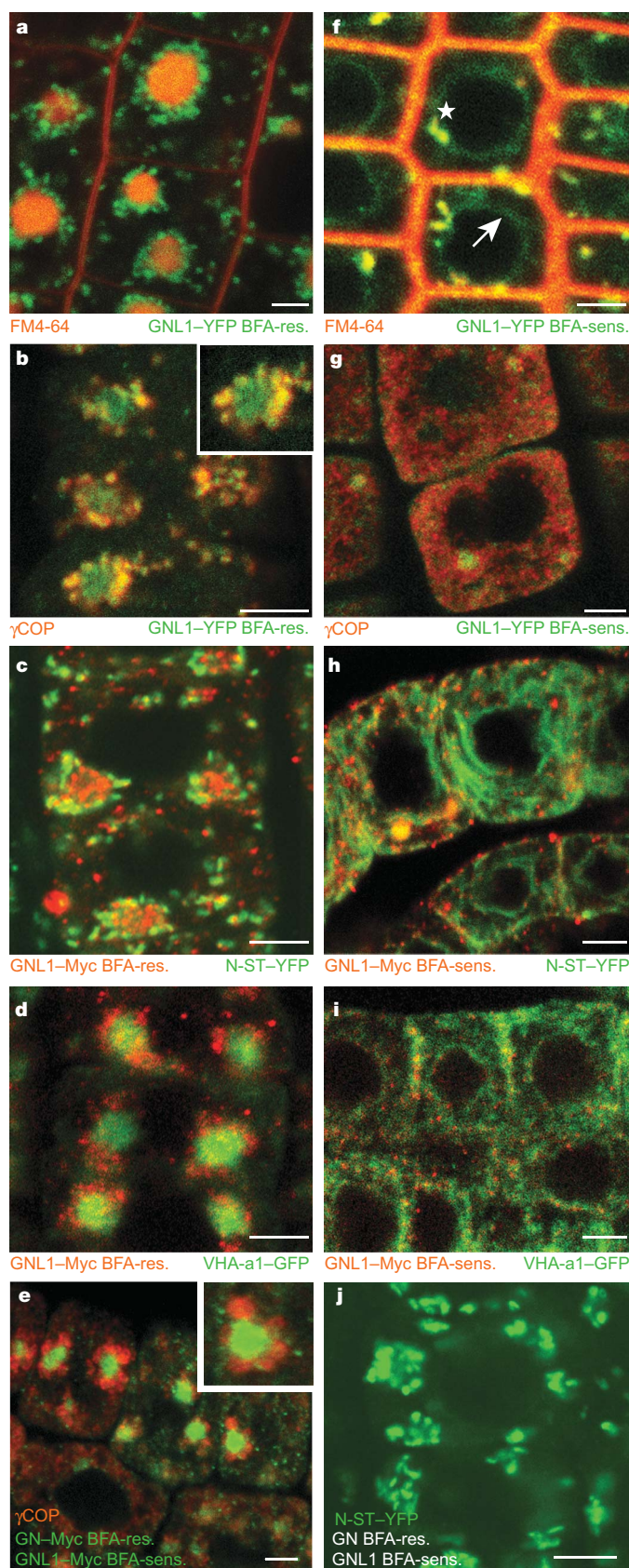


**Figure 2 | Localization of BFA-resistant and BFA-sensitive GNL1 after BFA treatment.** BFA-resistant (a–d) or BFA-sensitive (f–i) GNL1 in *gnl1* mutant background localized relative to compartment markers after BFA-treatment. **a, f**, Endocytic tracer FM4-64 (red) in BFA compartments colocalizes partially with GNL1-YFP and is surrounded by GNL1-YFP aggregates (a), whereas BFA-sensitive GNL1-YFP localizes to ER (arrow) and colocalizes with FM4-64 in small BFA compartments (f, asterisk). **b, g**, Golgi marker  $\gamma$ COP (red) partially overlaps with GNL1-YFP (b) but is released into the cytosol when GNL1-YFP is BFA-sensitive (g). **c, h**, Golgi marker N-ST-YFP (green) colocalizes partially with GNL1-Myc (c) but relocates to the ER when GNL1-Myc is BFA-sensitive (h). **d, i**, TGN marker VHA-a1-GFP (green) accumulates in BFA compartments (d) but is trapped in the ER when GNL1-Myc is BFA-sensitive (i). **e, j**, Golgi localization of  $\gamma$ COP (e, red) and N-ST-YFP (j, green) restored by BFA-resistant GN in BFA-sensitive GNL1, *gnl1* mutant background. All scale bars, 4  $\mu$ m.

that another, BFA-sensitive ARF-GEF is also involved in ER–Golgi trafficking (Fig. 3c, d; Supplementary Fig. 3e). One candidate would be GNOM, although GNOM is involved in endosomal recycling<sup>4</sup>. In addition, *gnom* mutant embryo cells did not display major Golgi abnormalities (Supplementary Fig. 3c) and GNOM did not co-localize with GNL1 (Fig. 3e). However, when both ARF-GEFs were

rendered either BFA-resistant or BFA-sensitive they co-localized partially or completely, respectively, after BFA treatment (Fig. 3f, g). In addition, the BFA-resistant form of both ARF-GEFs also co-localized partially with  $\gamma$ COP, suggesting the additional presence of GNOM protein at Golgi stacks (Figs 3h and 2b). To determine whether GNOM can substitute for GNL1 function, we analysed the localization of  $\gamma$ COP and N-ST-YFP in BFA-treated BFA-sensitive GNL1, *gnl1* mutant plants expressing engineered BFA-resistant GNOM (Fig. 2e, j). Surprisingly, the wild-type localization of the two markers was restored, although the BFA sensitivity of the two ARF-GEFs was reversed, indicating that BFA-resistant GNOM could compensate for the inactivation of BFA-sensitive GNL1 (Fig. 2e, j, compare with Fig. 2b, g and 2c, h, respectively). Thus, although GNOM might play only a minor part in ER–Golgi trafficking, it can take over the Golgi function of GNL1.

We also tested whether GNL1 can replace GNOM in the PIN1 endosomal recycling required for polar localization of PIN1 at the plasma membrane<sup>4</sup> (Fig. 4a–d). Polar targeting of PIN1 to the plasma membrane was only observed in BFA-treated seedlings when GNOM was BFA-resistant, regardless of BFA resistance or sensitivity of GNL1 (Fig. 4b, d). Thus, GNL1 has no obvious role in endosomal recycling. Interestingly, the BFA compartments were very small when both GNL1 and GNOM were BFA-sensitive, but attained their normal size when one or the other ARF-GEF was BFA-resistant. This suggests that BFA compartments are formed from both GNL1-dependent secretory and endocytic membrane material, although we cannot rule out a minor contribution of GNL1 to PIN1 recycling (compare Fig. 4c with 4a, d).

The capacity of GNOM to replace GNL1 cellular function could account for the observed, weak *gnl1* mutant phenotypes (Fig. 3i). Indeed, *gnl1 gnom* double mutants lacking both ARF-GEF activities were gametophytic lethal (Supplementary Table 2). This indicates that both ARF-GEFs are functionally redundant and that their double knockout affects some fundamental cellular function that leads to lethality even before fertilisation. Interestingly, other allele combinations with reduced ARF-GEF activity were also lethal, suggesting that the combined level of activity is critical (Supplementary Table 2). To determine their requirements in diploid somatic cells, both *GNL1* and *GNOM* were simultaneously downregulated by RNA interference (RNAi) expression (Supplementary Fig. 7b, c). The RNAi(*GNL1, GN*) expressing seedlings eventually died after 10–12 days of growth (Fig. 3j). Their ultrastructural analysis revealed abnormalities of the Golgi stacks, supporting our notion that ER–Golgi trafficking requires ARF-GEF function provided by both GNL1 and GNOM (Supplementary Fig. 3b).

To examine whether there are additional non-overlapping functions of GNL1 and GNOM, we performed promoter swaps and analysed the chimaeric genes for their ability to replace the two mutated genes. Surprisingly, *GNL1-GNOM* was able to rescue both *gnom* and *gnl1* mutants, whereas *GNOM-GNL1* only rescued *gnl1* but not *gnom* mutants (Fig. 4e; Supplementary Fig. 8a–c). Thus, GNOM and GNL1

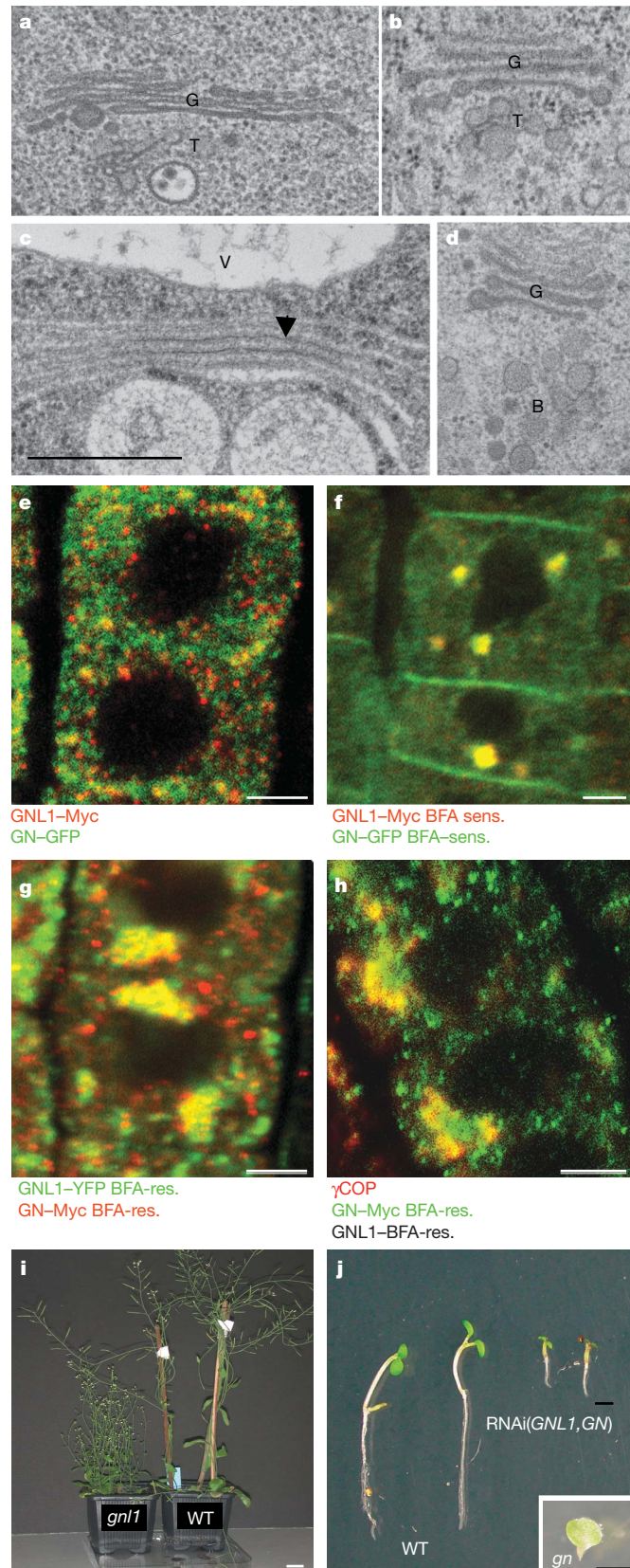


**Figure 3 | Phenotype of *gnl1* mutants and relationship of GNL1 to GN.**

**a–d**, Golgi morphology of *gnl1* mutant (**a**, **c**) in comparison to wild-type (**b**, **d**) after BFA treatment (**c**, **d**). **a**, **b**, Golgi of *gnl1* mutant (**a**) laterally expanded compared to wild-type in untreated controls. **c**, **d**, After 50  $\mu$ M BFA for 1 h, Golgi fuses with ER (arrowhead) in *gnl1* mutant (**c**), whereas Golgi morphology is retained in wild type (**d**). B, BFA compartment; G, Golgi; T, TGN; V, vacuole. Scale bar for **a–d**, 500 nm. **e–g**, Subcellular localization of GNL1 and GN. **e**, No colocalization of GNL1–Myc (red) with GN–GFP (green) in untreated cells. Nearly complete colocalization of BFA-sensitive versions in *gnl1* mutant (**f**) and partial colocalization of BFA-resistant versions (**g**) after BFA treatment. **h**, Partial colocalization of BFA-resistant GN with Golgi marker  $\gamma$ COP. Scale bars for **e–h**, 4  $\mu$ m. **i**, **j**, Phenotype of *gnl1* mutant plants and RNAi(*GNL1, GN*) seedlings. **i**, *gnl1* mutant plant (*gnl1*; left), wild type (WT; right). Scale bar, 2 cm. **j**, Seedling phenotypes of *RPS5A*-RNAi(*GNL1, GN*) (right) compared with wild type (left), 6 days after germination. Inset, *gn* mutant. Scale bar, 2 mm.

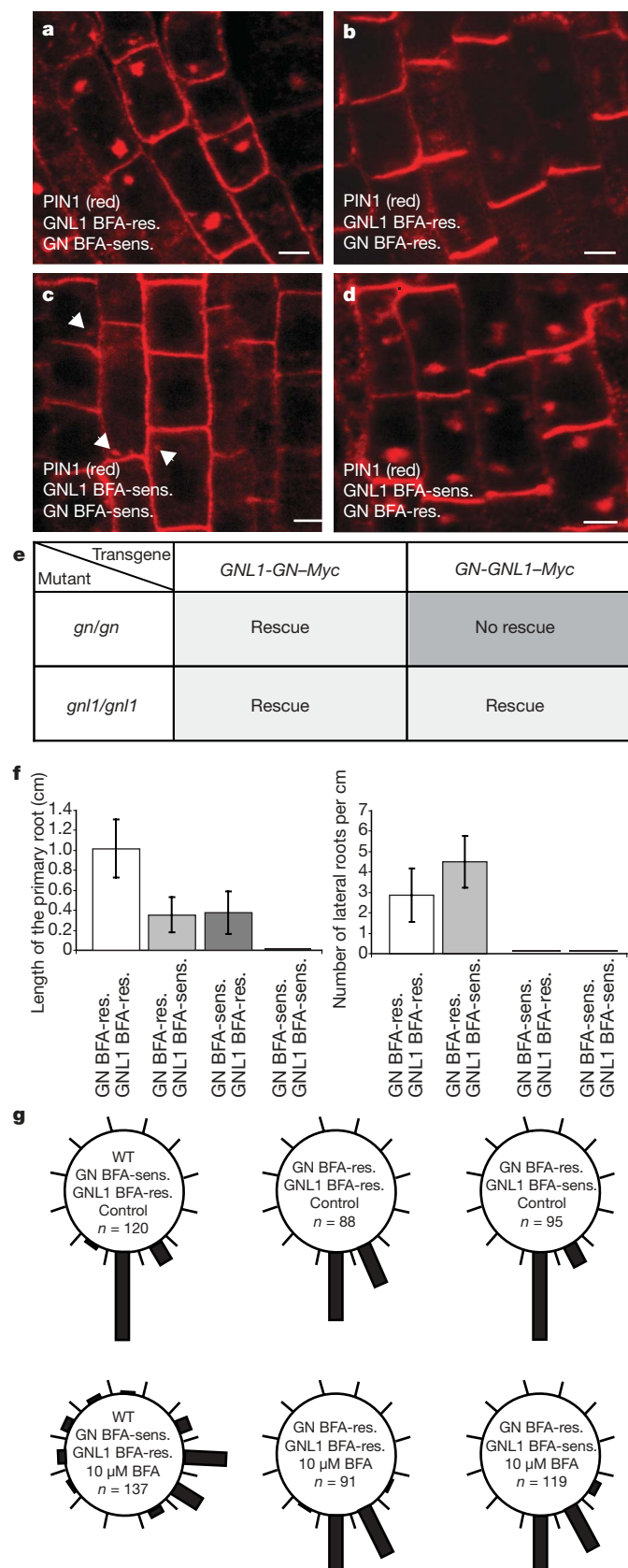


**Figure 4 | Functional relationship between GN and GNL1.** **a–d**, PIN1 localization after BFA treatment. **a**, GN BFA-sensitive, GNL1 BFA-resistant (wild type): PIN1 is localized in BFA compartments and symmetrically at the plasma membrane. **b, d**, Polar localization of PIN1 at the plasma membrane and variable accumulation of PIN1 in BFA compartments when only GN (**b**) or both GN and GNL1 (**d**) are BFA-resistant. **c**, GN and GNL1 BFA-sensitive in *gnl1* mutant background: PIN1 is localized in very small BFA compartments (arrowheads) and symmetrically at the plasma membrane (similar to wild type, Fig. 4a). Scale bars for **a–d**, 4  $\mu$ m. **e**, Promoter swaps between *GN* and *GNL1* suggest asymmetric functional redundancy. **f, g**, Seedlings expressing different combinations of BFA-resistant (res.) versus BFA-sensitive (sens.) GNL1 and GNOM (*GN*) in *gnl1* mutant background (except for wild-type) were treated with BFA. **f**, Left panel, additive effects of GNL1 and GN in primary root growth. Right panel, lateral root formation is mainly dependent on GN but not on GNL1. Error bars indicate standard deviation;  $n = 46$  (GN BFA-res., GNL1 BFA-res.), 46 (GN BFA-res., GNL1 BFA-sens.), 22 (GN BFA-sens., GNL1 BFA-res., which corresponds to wild type), 25 (GN BFA-sens., GNL1 BFA-sens.). **g**, Root gravitropism is a GN-dependent process (upper panel, control; lower panel, BFA treatment).

initiation and root gravitropism. The two ARF-GEFs acted interchangeably in seed germination (Supplementary Fig. 9). Unexpectedly, expression of either BFA-resistant ARF-GEF, GNL1 or GNOM, was sufficient to sustain root growth at half the rate of roots expressing both BFA-resistant ARF-GEFs, indicating that primary root growth requires both GNL1 and GNOM function (Fig. 4f, left). In contrast, both lateral root initiation and root gravitropism were dependent on BFA-resistant GNOM, whereas BFA sensitivity or resistance of GNL1 had no effect of its own (Fig. 4f, right; 4g). This requirement for GNOM-specific ARF-GEF function is related to its role in endosomal recycling of PIN1 (ref. 4, 22).

Our results offer a surprising explanation for why ARF-GEFs of the GBF1 clade act in different trafficking pathways in plants than in mammals or yeast. There are two closely related ARF-GEFs, GNL1 and GNOM, that share the ancestral Golgi-associated function of GBF1-type ARF-GEFs in *Arabidopsis* and probably in other flowering plants as well (Supplementary Fig. 1). This was not noticed before because, unlike in mammals, there was no BFA effect on the localization of  $\gamma$ COP in wild-type *Arabidopsis*, although GNOM is BFA-sensitive<sup>4,14</sup>. In contrast, a rapid effect of BFA on the Golgi morphology and the localization of  $\gamma$ COP was described for tobacco BY-2 cells<sup>23</sup>, suggesting that the tobacco GNL1 orthologue is BFA-sensitive. Indeed, we found a BFA-sensitive signature for the rice putative orthologue of GNL1 (Supplementary Fig. 10). Our data imply that the Golgi-localized ARF-GEF function is ancestral and conserved among eukaryotes, although the plant lineage has apparently undergone gene duplication such that two closely related ARF-GEFs perform the GBF1-equivalent function. GNOM acquired an additional specific function in endosomal recycling of plasma membrane proteins that is not shared by GNL1. Unlike plants, animals have evolved new classes of small or medium-sized ARF-GEFs named cytohesin, EFA and BRAG, which are involved in endosomal trafficking<sup>5</sup>. In addition, a member of the BIG class of large ARF-GEFs named BIG2 acts not only at the TGN, like its close relative BIG1, but also at recycling endosomes<sup>24</sup>. Thus, the elaboration of post-Golgi trafficking seems to have evolved independently in the two major multicellular lineages, whereas the regulation by ARF-GEF of ER–Golgi traffic was already in place in unicellular eukaryotes.

## METHODS SUMMARY

**Molecular biology.** For expression of tagged GNL1, a complementing genomic fragment was transformed into *gnl1* mutants, and BFA sensitivity was engineered by replacing methionine with leucine in the SEC7 domain. For RNAi(*GN*, *GNL1*) analysis, fragments of *GNL1* and *GN* coding sequence in tandem in sense and antisense direction were introduced into a two-component vector for expression by *RPS5A-GALA* activator<sup>25</sup>. Transcript levels were analysed by RT–PCR. Promoter swaps involved 2-kb promoter fragments and were introduced into *gnl1* and *emb30-1* (ref. 8) heterozygous plants.

share one common, essential function in ER–Golgi trafficking, whereas only GNOM has another, unique essential function in endosomal recycling.

We then used BFA to determine the relative contributions of GNL1 and GNOM in different BFA-sensitive developmental processes such as seed germination, primary root growth, lateral root

**Expression analysis.** Protein blots<sup>26</sup>, immunofluorescence localization<sup>4,26,27</sup>, FM4-64 staining<sup>4</sup>, BFA treatment<sup>4</sup>, immunolocalization on cryosections<sup>28</sup>, electron microscopy<sup>28</sup> and physiological tests<sup>4</sup> were performed as described.

**Bioinformatics.** An unrooted phylogenetic tree of SEC7 domains from different ARF-GEFs was derived from sequence alignment using ClustalW ([www.ebi.ac.uk/clustalw](http://www.ebi.ac.uk/clustalw)).

**Full Methods** and any associated references are available in the online version of the paper at [www.nature.com/nature](http://www.nature.com/nature).

**Received 18 February; accepted 30 May 2007.**

- Shin, H. W. & Nakayama, K. Guanin nucleotide-exchange factors for arf GTPases: their diverse functions in membrane traffic. *J. Biochem.* **136**, 761–767 (2004).
- Zhao, X. *et al.* GBF1, a cis-Golgi and VTCs-localized ARF-GEF, is implicated in ER-to-Golgi protein traffic. *J. Cell Sci.* **119**, 3743–3753 (2006).
- Peyroche, A., Courbeyrette, R., Rambourg, A. & Jackson, C. L. The ARF exchange factors Gea1p and Gea2p regulate Golgi structure and function in yeast. *J. Cell Sci.* **114**, 2241–2253 (2001).
- Geldner, N. *et al.* The *Arabidopsis* GNOM ARF-GEF mediates endosomal recycling, auxin transport, and auxin-dependent plant growth. *Cell* **112**, 219–230 (2003).
- Cox, R., Mason-Gamer, R. J., Jackson, C. L. & Segev, N. Phylogenetic analysis of Sec7-domain-containing Arf nucleotide exchangers. *Mol. Biol. Cell* **15**, 1487–1505 (2004).
- Mouratou, B. *et al.* The domain architecture of large guanine nucleotide exchange factors for the small GTP-binding protein Arf. *BMC Genom.* **6**, 20 (2005).
- Spang, A., Herrmann, J. M., Hamamoto, S. & Schekman, R. The ADP ribosylation factor-nucleotide exchange factors Gea1p and Gea2p have overlapping, but not redundant functions in retrograde transport from the Golgi to the endoplasmic reticulum. *Mol. Biol. Cell* **12**, 1035–1045 (2001).
- Mayer, U., Büttner, G. & Jürgens, G. Apical-basal pattern formation in the *Arabidopsis* embryo: studies on the role of the *gnom* gene. *Development* **117**, 149–162 (1993).
- Steinmann, T. *et al.* Coordinated polar localization of auxin efflux carrier PIN1 by GNOM ARF GEF. *Science* **286**, 316–318 (1999).
- Cherfils, J. & Melançon, P. On the action of Brefeldin A on Sec7-stimulated membrane-recruitment and GDP/GTP exchange of Arf proteins. *Biochem. Soc. Trans.* **33**, 635–638 (2005).
- Peyroche, A. *et al.* Brefeldin A acts to stabilize an abortive ARF–GDP–Sec7 domain protein complex: involvement of specific residues of the Sec7 domain. *Mol. Cell* **3**, 275–285 (1999).
- Barzilay, E., Ben-Califa, N., Hirschberg, K. & Neumann, D. Uncoupling of brefeldin A-mediated coatomer protein complex-I dissociation from Golgi redistribution. *Traffic* **6**, 794–802 (2005).
- Niu, T. K., Pfeifer, A. C., Lippincott-Schwartz, J. & Jackson, C. L. Dynamics of GBF1, a Brefeldin A-sensitive Arf1 exchange factor at the Golgi. *Mol. Biol. Cell* **16**, 1213–1222 (2005).
- Geldner, N., Friml, J., Stierhof, Y.-D., Jürgens, G. & Palme, K. Auxin transport inhibitors block PIN1 cycling and vesicle trafficking. *Nature* **413**, 425–428 (2001).
- Schmid, M. *et al.* A gene expression map of *Arabidopsis thaliana* development. *Nature Genet.* **37**, 501–506 (2005).
- Pimpl, P. *et al.* *In situ* localization and *in vitro* induction of plant COPI-coated vesicles. *Plant Cell* **12**, 2219–2236 (2000).
- Dettmer, J., Hong-Hermesdorf, A., Stierhof, Y.-D. & Schumacher, K. Vacuolar H<sup>+</sup>-ATPase activity is required for endocytic and secretory trafficking in *Arabidopsis*. *Plant Cell* **18**, 715–730 (2006).
- Ueda, T., Uemura, T., Sato, M. H. & Nakano, A. Functional differentiation of endosomes in *Arabidopsis* cells. *Plant J.* **40**, 783–789 (2004).
- Lee, G. J., Sohn, E. J., Lee, M. H. & Hwang, I. The *Arabidopsis* rab5 homologs Rha1 and Ara7 localize to the prevacuolar compartment. *Plant Cell Physiol.* **45**, 1211–1220 (2004).
- Grebe, M. *et al.* *Arabidopsis* sterol endocytosis involves actin-mediated trafficking via ARA6-positive early endosomes. *Curr. Biol.* **13**, 1378–1387 (2003).
- Teh, O. & Moore, I. An ARF-GEF acting at the Golgi and in selective endocytosis in polarized plant cells. *Nature* doi:10.1038/nature06023 (this issue).
- Geldner, N. *et al.* Partial loss-of-function alleles reveal a role for GNOM in auxin transport-related, post-embryonic development of *Arabidopsis*. *Development* **131**, 389–400 (2004).
- Ritzenthaler, C. *et al.* Reevaluation of the effects of brefeldin A on plant cells using tobacco Bright Yellow 2 cells expressing Golgi-targeted green fluorescent protein and COPI antisera. *Plant Cell* **14**, 237–261 (2002).
- Shin, H. W., Morinaga, N., Noda, M. & Nakayama, K. BIG2, a guanine nucleotide exchange factor for ADP-ribosylation factors: its localization to recycling endosomes and implication in the endosome integrity. *Mol. Biol. Cell* **15**, 5283–5294 (2004).
- Weijers, D., Van Hamburg, J. P., Van Rijn, E., Hooykaas, P. J. & Offringa, R. Diphtheria toxin-mediated cell ablation reveals interregional communication during *Arabidopsis* seed development. *Plant Physiol.* **133**, 1882–1892 (2003).
- Lauber, M. H. *et al.* The *Arabidopsis* KNOLLE protein is a cytokinesis-specific syntaxin. *J. Cell Biol.* **139**, 1485–1493 (1997).
- Müller, A. *et al.* AtPIN2 defines a locus of *Arabidopsis* for root gravitropism control. *EMBO J.* **17**, 6903–6911 (1998).
- Völker, A., Stierhof, Y.-D. & Jürgens, G. Cell cycle-independent expression of the *Arabidopsis* cytokinesis-specific syntaxin KNOLLE results in mistargeting to the plasma membrane and is not sufficient for cytokinesis. *J. Cell Sci.* **114**, 3001–3012 (2001).
- Rios, G. *et al.* Rapid identification of *Arabidopsis* insertion mutants by non-radioactive detection of T-DNA tagged genes. *Plant J.* **32**, 243–253 (2002).
- Vieten, A. *et al.* Functional redundancy of PIN proteins is accompanied by auxin-dependent cross-regulation of PIN expression. *Development* **132**, 4521–4531 (2005).
- Song, J., Lee, M. H., Lee, G. J., Yoo, C. M. & Hwang, I. *Arabidopsis* EPSIN1 plays an important role in vacuolar trafficking of soluble cargo proteins in plant cells via interactions with clathrin, AP-1, VTI11, and VSR1. *Plant Cell* **18**, 2258–2274 (2006).

**Supplementary Information** is linked to the online version of the paper at [www.nature.com/nature](http://www.nature.com/nature).

**Acknowledgements** We thank N. Takada and L. Müller for technical assistance, A. Vieten, J. Friml, F. El-Kasmi, G. Strompen and K. Steinborn for screening the Cologne T-DNA insertion lines, K. Schumacher, I. Hwang, M. Grebe, A. Schlereth and D. Weijers for providing materials, O. Teh and I. Moore for sharing unpublished material and results, and N. Anders, U. Mayer, K. Schumacher and D. Weigel for critically reading the manuscript and suggestions. We especially thank N. Anders for advice and discussions. This work was supported by an EMBO long-term Fellowship to J.S. and by grants from the Human Frontier in Science Program Organization and the SFB 446 of the Deutsche Forschungsgemeinschaft to G.J.

**Author Contributions** S.R. carried out most of the experiments, N.G. initiated the project, J.S. generated the RNAi and promoter-swap lines, H.W. generated the ARA7–GFP marker line, Y.-D.S. performed the electron microscopy analysis and immunogold localization experiments, G.R. and C.K. provided the T-DNA collection, D.G.R. generated antisera against markers, and G.J. and S.R. designed the experiments, discussed the results and wrote the manuscript.

**Author Information** Reprints and permissions information is available at [www.nature.com/reprints](http://www.nature.com/reprints). The authors declare no competing financial interests. Correspondence and requests for materials should be addressed to G.J. ([gerd.juergens@zmbp.uni-tuebingen.de](mailto:gerd.juergens@zmbp.uni-tuebingen.de)).

## METHODS

**Plant material and growth conditions.** *Arabidopsis* wild-type (ecotype Col-0) and mutant lines carrying *gnom* alleles *R5* (ref. 22) or *emb30-1* (ref. 8) have been described. Plant growth conditions were as described<sup>22</sup>. Seedlings (Col-0 ecotype) were grown from surface-sterilized seeds on vertical agar plates at 24 °C for 5 days under long day conditions<sup>22</sup>.

***gnl1* mutant.** The *gnl1-1* T-DNA insertion line (ecotype Col-0) was isolated as described<sup>29</sup>. The T-DNA insertion is located in the first exon at 102 base pairs downstream of the ATG and confers hygromycin resistance. The plants were selected on plates containing 15 µg ml<sup>-1</sup> hygromycin (Gibco). The genotype was characterized by two PCRs: one to detect the T-DNA insertion (sense primer, 5'-GATTGAGCCAAGAAGTTGGGGCGAG-3'; antisense primer, 5'-CTGGGAA-TGGCGAAATCAAGGCAT-3'), another to amplify the wild-type gene sequence spanning the T-DNA insertion site (sense primer, 5'-ACAAAAGGGTA-GAGTTGAAAAGGG-3'; antisense primer: 5'-TACATTTCTCCTCATCACAGCCAAA-3').

**Generating transgenic plants.** An 8.8-kb genomic *GNL1* fragment containing 2-kb of 5' UTR and 1-kb of 3' UTR from BAC clone MUL8 complemented the *gnl1* mutant phenotype. Primer-extension PCR was used to insert 3 × Myc or YFP tag at the C-terminus as well as to introduce the leucine 696 (TTG) to methionine 696 (ATG) mutation in the SEC7 domain. All constructs were transformed into *gnl1/GNL1* heterozygous plants, and at least five *gnl1* mutant lines each were established for BFA-resistant and BFA-sensitive *GNL1* transgenes and shown to complement the bushy plant phenotype of *gnl1* mutants.

For RNAi (*GN*, *GNL1*) analysis, 172 bp of *GNL1* and 162 bp of *GNOM* coding sequence were cloned in tandem in sense and antisense orientation, introduced into the *UAS* vector of the *GAL4* >> *UAS* two-component expression system and transformed into Col-0 plants. T<sub>2</sub> plants were crossed with *RPS5A-GAL4* plants<sup>25</sup>, and the F<sub>1</sub> seedling progeny with abnormal phenotypes were analysed.

A 2-kb promoter fragment of *GNL1* and a 2.1-kb promoter fragment of *GN* were fused to genomic fragments for promoter swapping. These constructs were introduced into *gnl1/GNL1* as well as *emb30-1/GN* heterozygous plants<sup>8</sup>.

All T<sub>1</sub> plants were selected by spraying seedlings on soil with BASTA (1:1,000; AgrEvo) or by adding kanamycin (50 µg ml<sup>-1</sup>; Sigma) to plates.

**Immunofluorescence localization.** Five-day-old seedlings were incubated in 1 ml of liquid growth medium (×0.5 MS medium, 1% sucrose, pH 5.8) containing 50 µM BFA (Invitrogen, Molecular Probes) for 1 h (or, 100 µM for 2 h in double labelling for GN and GNL1) at room temperature in 24-well cell-culture plates. Incubation was stopped by fixation with 4% paraformaldehyde in MTSB. Immunofluorescence staining was performed as described<sup>26</sup> or with an InsituPro machine (Intavis)<sup>27</sup>.

Antibodies used were: mouse anti-c-Myc mAb 9E10 (Santa Cruz Biotechnologies) diluted 1:600; mouse anti-GFP (Roche) 1:600; rabbit anti-GFP (Invitrogen, Molecular Probes) 1:600; rabbit anti-PIN1 (ref. 30) 1:1,000; rabbit anti-AtγCOP (ref. 16) 1:1,000; and anti-clathrin<sup>31</sup> 1:500. FITC or Cy3-conjugated secondary antibodies (Dianova) were diluted 1:600.

Epitope-tagged or GFP-fusion markers were transformed or crossed into tagged *GNL1* lines: *RPS5A-GFP-ARA7* (ref. 18) (GFP-ARA7; cloned into pGrIIK RPS5a-tNOS; ref. 25), VHA-a1-GFP<sup>17</sup>, N-ST-YFP<sup>20</sup>, GN-3 × Myc<sup>4</sup> (BFA-sensitive and resistant) and BFA-sensitive GN-GFP<sup>4</sup>.

Fluorescence signals of GFP- or YFP-tagged proteins were enhanced by staining with anti-GFP antibody in fixed cells. Live cell imaging was performed with 2 µM FM4-64 (Invitrogen, Molecular Probes).

**Acquisition and processing of fluorescence images.** Fluorescence images were acquired at 512 × 512 pixels with the confocal laser scanning microscope TCS-SP2 from Leica, using the ×63 water-immersion objective and Leica software. All images were processed with Adobe Photoshop CS2 only for adjustment of contrast and brightness.

**Immunolocalization on cryosections, and electron microscopy.** Ultrastructural analysis of high-pressure frozen, freeze-substituted and resin-embedded root tips and embryos, and immunogold labeling using silver-enhanced Nanogold (Nanoprobes, USA) of ultrathin cryosections were carried out as described<sup>17</sup>.

**Physiological tests.** To investigate primary root growth and lateral root formation, 5-day-old seedlings were transferred to plates with 20 µM BFA and analysed after 7 additional days.

For measurement of gravitropic responses, 4-day-old seedlings were transferred to plates containing 10 µM BFA. After 1 day, the plates were turned by 135°. Pictures were taken 12 h later and deviation from the gravity vector was measured.

For the germination assay, surface-sterilized seeds were plated on agar plates (×0.5 MS medium, 1% sucrose, pH 5.8) containing 20 µM BFA. After two days of stratification, the plates were incubated at 23 °C for 4 days before seed germination rates were determined.

**Analysis of transcript levels in *gnl1* mutants and RNAi (*GN*, *GNL1*) lines.** RNA isolation was performed using Plant RNAeasy Kit from Qiagen. RT-PCR was done with Revert Aid H Minus First Strand cDNA Synthesis Kit (Fermentas). PCR on *gnl1* cDNA from plants was performed with sense primer 5'-CTGGGAATGGCGAAATCAAGGCAT-3' and antisense primer 5'-CTTTTT-TCTCCAGAATTCGG-3'. PCR on cDNA from RNAi seedlings was done with sense primer 5'-GTGCAGTTTTGGCTGTGATG-3' and antisense primer 5'-CTTTTTTCTCCAGAAATTCGG-3' to investigate *GNL1* transcript level. For *GN*, sense primer 5'-TACACTTGTC AACAGAGCTGGTAGC-3' and antisense primer 5'-TCTGTCATTATATGCAAATCATATGGAGAAGCCG-3' were used.

**Western blot analysis.** Five-day-old seedlings were used for protein extraction<sup>26</sup>. Protein extracts were loaded onto a 12% polyacrylamide gel and transferred onto a PVDF membrane. Rabbit anti-GNOM (SEC7) antiserum diluted 1:2,000 and anti-rabbit horseradish peroxidase (POD)-conjugated secondary antibody (Roche) 1:5,000 were used to detect endogenous GNOM protein. Detection was performed with BM chemiluminescence blotting substrate (Roche).

**Phylogenetic tree.** SEC7 domain sequences of ARF-GEFs from different species, corresponding to the GN SEC7 domain, were aligned by ClustalW (www.ebi.ac.uk/clustalw) and the phylogenetic tree was drawn with TreeViewer.